Available online at www.sciencedirect.com
SCIENCE DIRECT®
Polymer 44 (2003) 7449–7457
polymer
www.elsevier.com/locate/polymer

Nanocomposites based on a combination of epoxy resin, hyperbranched epoxy and a layered silicate

D. Ratna[a], O. Becker[b], R. Krishnamurthy[b], G.P. Simon[b,*], R.J. Varley[c]

[a]*Naval Materials Research Laboratory, Chickloli, Anandanagar P.O Addl. Ambernath (E), Thane 421 506, India*
[b]*School of Physics and Materials Engineering, Monash University, Clayton, Vic. 3800, Australia*
[c]*CSIRO, Molecular Science, Clayton, Vic. 3168, Australia*

Received 20 March 2003; received in revised form 16 June 2003; accepted 21 August 2003

Abstract

Epoxy/clay nanocomposites have been prepared using an diglycidyl ether of bisphenol A (DGEBA) epoxy and its blend with an epoxy functionalized hyperbranched polymer (HBP). The formation of nanocomposites was confirmed by a wide angle X-ray diffraction (WAXD) and transmission electron microscopy (TEM) analysis. The mechanical and dynamic mechanical properties of the nanocomposites were evaluated and compared with the corresponding matrix. The improvement in impact properties in blend and nanocomposites was explained in terms of fracture surface analysis by scanning electron microscopy (SEM).
© 2003 Published by Elsevier Ltd.

Keywords: Epoxy; Nanocomposite; Rubber

1. Introduction

Nanostructured hybrid organic–inorganic composites have attracted considerable attention in recent years, both with regards to basic research and from an application point of view [1–3]. Generally composite materials are formed when at least two distinctly dissimilar materials are combined, the overall properties determined not only by those of the components, but also by the composite phase morphology and interfacial properties. A nanocomposite is formed when at least one of the phases has a size scale of the order of nanometres and is sufficiently dispersed so that this level of intimacy is realised. Nanocomposites usually exhibit improved performance properties compared to conventional composites, due to their unique phase morphology and high surface area [4]. One successful approach to achieve such nanocomposites is the in situ polymerization of metal alkoxides in organic matrices via the sol–gel process. Inorganic components, especially silica have been formed by the hydrolysis and condensation of a mononuclear precursor such as tetraethoxysilane (TEOS) in many polymer systems [5–8]. Owing to the loss of volatile byproducts formed in the hydrolysis/condensation reaction, it is difficult to control sample shrinkage after molding.

Pioneering work by researcher at Toyota led to the discovery of nanoscale polymer–clay hybrid composites for lightweight material applications [9,10]. By replacing the hydrophilic sodium cations of native montmorillonite with more hydrophobic onium ions, they were able to initiate polymerization of caprolactam in the interlayer gallery of the montmorillonite galleries to form a nylon 6-clay nanocomposite. Since the clay layers are of the order of 1 nm thick, they can either have polymer molecules (one or two wide) residing inside the galleries (intercalation), or the whole stack of clay layers can be delaminated (exfoliation). Often a combination of both is found, with regions known as tactoids occurring, where the clay layers have been pushed apart by tens of angstroms or more, but some lateral registration of clay order still exists. Following the initial work on nylon 6, efforts have been made to develop nanocomposites using many polymer matrices, by such in situ (polymerisation) intercalation as with nylon, as well as more recently by melt intercalation [11–14]. The latter technique allows a much broader range of nanocomposites to be made from differing materials, by conventional processing techniques. Epoxy materials have been of particular interest, many clay/epoxy/catalyst systems

* Corresponding author. Tel.: +61-3-99054936; fax: +61-3-99054940.
E-mail address: george.simon@spme.monash.edu.au (G.P. Simon).

0032-3861/$ - see front matter © 2003 Published by Elsevier Ltd.
doi:10.1016/j.polymer.2003.08.035

showing either intercalation and/or exfoliation, and improvement in properties such as modulus and strength [15,16] with a possible combination of other useful properties such as improved flame retardance [17] and reduced gas and moisture permittivity [18]. In general, in many systems in which modulus and strength is increased, a concomitant decrease in toughness is observed. However, improved toughness has also been seen in some epoxy/clay systems, and attributed in part, to the intercalated regions shearing during crack growth and increased crack surface area, leading to dissipation of energy [3,15].

Since most glassy epoxy materials are themselves intrinsically brittle, some form of toughening is often employed. This includes incorporation of materials such as liquid rubber which phase separates and improves toughness by a range of mechanisms such as increased yielding, cavitation, crack blunting and so forth. A downside of this is decreased modulus of the thermoset material due to the rubber particles, a problem often compounded by incomplete phase separation of the rubber which results in a lower glass transition temperature of the remaining rubber-plasticised matrix.

This paper presents results of a new strategy to produce toughened epoxy resins and maintain a high modulus. This involves a ternary blend—incorporation both of a rubbery phase and a rigid layered silicate phase into the epoxy. In this paper, a hyperbranched epoxy resin is used as the toughening phase. The use of this to increase the fracture toughness of epoxies in a binary mixture with epoxies has itself only been relatively recently reported [19]). The addition of silicate nanoparticles may help recover some of the rigidity lost due to addition of the toughening agents, and indeed may also contribute to improve toughness as well, as mentioned above. To date, we have not seen any reports of epoxy nanocomposites based on the ternary system of epoxy resin, toughening component and clay.

As well as extension into ternary systems, a number of the binary systems involved are also of some interest. The use of hyperbranched epoxy resins, rather than classical rubber materials, as the toughening agent is relatively new. This has recently been shown by others [19] and ourselves [20] to effectively toughen glassy epoxy matrices, phase-separating in the same manner as more conventional rubbers. The use of such a HBP with its highly branched, three dimensional structure and high concentration of end groups has the promise of good internal bonding rubber phase due to the presence of surface functional groups, in addition to low initial viscosity (small hydrodynamic volume). This paper also reports on the intercalation/exfoliation ability of the HBP alone with layered silicate. To the best of our knowledge, this binary system also has not been yet reported. The formation of nanocomposites using branched polymers has been recently predicted by molecular simulation to be highly favoured [21].

2. Experimental

2.1. Material

The epoxy resin used was a liquid diglycidyl ether of bisphenol A (DGEBA) (DER 331 Dow epoxy resin) containing 5.27 mmol epoxide per gram of resin. Ethacure 100 of Albemarle Corporation, USA, was used as a curing agent and is a mixture of the two diethyltoluene diamine (DETDA) isomers (74–80% 2,4 isomer and 18–24% 2,6 isomer). The chemical structures of the epoxy resin and hardener are shown in Fig. 1.

The epoxy functional dendritic hyperbranched polymer (Boltorn E1) with an epoxy equivalent weight of ~875 g/equiv. and a molecular weight of ~10500 g/mol, was supplied by Perstorp Specialty Chemicals, Sweden. Boltorn E1 consists of a highly branched aliphatic polyester backbone with an average of 11 reactive epoxy groups per molecule. A schematic illustration of HBP is also shown in Fig. 1.

The clay used for synthesis of nanocomposite was a commercial treated clay I.30E (Nanocor, USA) which contains octadecylammonium organo-ions lining the surface of the galleries, encouraging ingress of the monomer and hardener.

2.2. Preparation of epoxy-nanocomposites

All chemicals were dried at 60 °C under vacuum prior to sample preparation. DGEBA resin and DGEBA/HBP blend containing 15% HBP were used as matrices. The organically modified clay was dispersed in the DGEBA resin or blend at 80 °C using a Janke and Kunkel Labortechnik stirrer at 500 rpm at a concentration of 5 wt% ratio. After stirring for 45 min, a stoichiometric amount of curing agent was added and mixed under vacuum for another 30–40 min at 100 °C. The mixture was than sonicated for 10 min to encourage initial ingress into the clay of monomer and to remove bubbles and poured into moulds. Curing was performed for 2 h at 100 °C, 1 h at 130 °C and 2 h at 200 °C.

2.3. Mechanical thermal analysis (DMTA)

Dynamic mechanical thermal analysis (OHTA) of solid, cured epoxy samples was done by a Dynamic Mechanical Thermal Analyzer (DMTA MK IV, Rheometric Scientific) at a fixed frequency of 1 Hz with 3 °C/min heating rate using liquid nitrogen for subambient region. Dynamic moduli and loss factors were obtained by dual cantilever mode for the sample of size $45 \times 10 \times 2$ mm^3.

The dynamic mechanical properties of the unreacted HBP liquid were also required, and to carry this out a Perkin Elmer DMA7 was also used in the penetration probe configuration. This DMTA has the advantage of applying a cyclical oscillation to a downward-thrusting probe. If a liquid sample is contained in a small vessel, such as a DSC

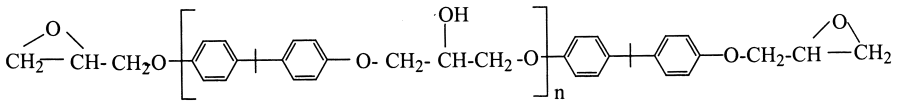

DGEBA

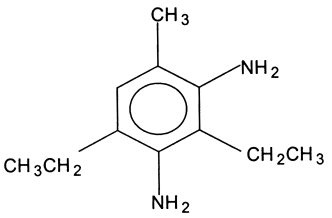

3,5-Diethyltoluene-2,4-diamine

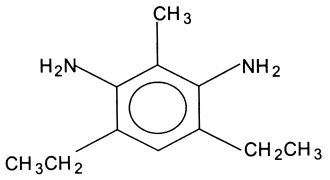

3,5-Diethyltoluene-2,6-diamine

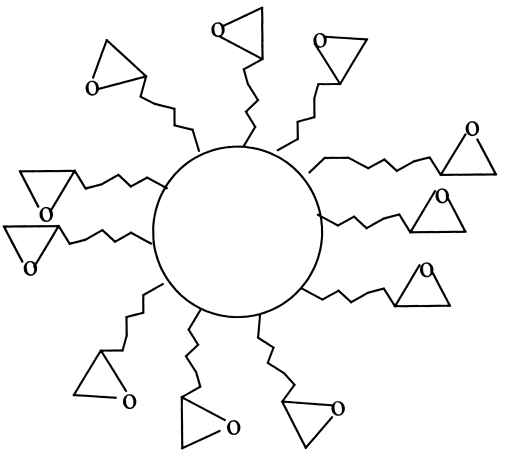

HBP

Fig. 1. Chemical structures of epoxy resin, curing agent and HBP.

pan, then the sample can be cooled and the glass transition readily obtained by thermal scanning and observing the loss tangent. A heat rate of 3 °C/min and a frequency of 1 Hz was also used.

2.4. Wide angle X-ray scattering

Wide angle X-ray diffraction (XRD) analysis was performed using a Rigaku Geigerflex generator with a wide-angle goniometer. An acceleration voltage of 40 kV and a current of 22.5 mA were applied using Ni filtered Cu Kα radiation.

2.5. Flexural test

Flexural properties (strength, modulus and strain) were measured with rectangular samples according to ASTM D-790, using a universal testing machine (UTM), Hounsfield, at a crosshead speed of 2 mm/min. The sample size was $120 \times 25 \times 2.5$ mm^3 and the results of three samples averaged for each material.

2.6. Impact test

Impact strength of the modified epoxy samples was determined by an instrumented falling dart impact tester (Radmana, ITR 2000). The annular hole on the specimen fixture was approximately 4 cm in diameter. The sample size used for the test was $80 \times 80 \times 5$ mm^3. The impact test was carried out at room temperature (25 °C) and impact energy (calculated from the area of the load vs. deformation curve) was reported in J/m. The quoted result is the average of the determination on four samples.

2.7. SEM analysis

A low voltage scanning electron microscope (SEM) (JEOL, JSM 840)) was used to examine the fracture surfaces of the toughened epoxy samples. A thin section of the fracture surface was cut and mounted on an aluminum stub using a conductive (silver) paint and was sputter coated with gold prior to fractographic examination. SEM photo micrographs were obtained under conventional secondary electron imaging conditions with an accelerating voltage of 20 kV.

2.8. TEM analysis

A JEOL 200CX transmission electron microscope was used at 200 kV to characterize the microtomed nanocomposite samples. The samples containing a rubbery HBP phase were cryo-microtomed to produce samples of around 0.3 μm whereas the rigid DGEBA and silicate material could be microtomed readily to 70 nm thicknesses at room temperature. All the images were taken in bright field imaging mode.

3. Results and discussion

For natural clays like montmorillonite, the cation residing in interlayer space are alkali and alkaline earth metals and thus mineral is hydrophilic. This results in a high interfacial tension with organic materials making the layered silicate difficult to intercalate and disperse homogeneously in a polymer matrix. Thus it is necessary to use a clay in which the hydrophilic ions are replaced by more organophilic alkyl-ammonium cations, commercial I.30E in this work. In order to confirm the formation of nanocomposite (partial or full delamination of the layers), the nanocomposites were subjected to WAXD analysis and compared with the clay. This is possible because the diffraction peak related to the stacking of the clay layers (the 001 peak) can be readily seen at low angles (usually between about $2\theta = 5-10°$). Movement of the peak to lower angles (greater d-spacings) implies intercalation, whereas if the peak cannot be observed, some level of exfoliation has occurred.

Fig. 2 shows X-ray analysis data of the virgin clay, the clay in DGEBA, clay in neat, cured HBP and the DGEBA/HBP/clay nanocomposite. The d_{001} peak in the clay occurs at angles of $2\theta = 3.85°$, corresponding to a d-spacing of 23 Å. The absence of d_{100} peak in the X-ray spectrum of all binary and ternary systems indicates exfoliation (as judged by this technique) in the HBP, DGEBA and in the DGEBA/HBP blend. It should be noted that the disappearance of the 001 peak is not due to dilution (low concentrations of clay). In other work, where less intercalation occurs, we do clearly see 001 peaks at these levels of addition. Further, peaks due to the crystalline structure of the layered silicates themselves (seen in line (a) of Fig. 2 at around 20°, also manifest as shoulders on the broad amorphous peak centered around 17°. The difficulty in seeing clearly distinguished peaks of the clay layers themselves at higher angles is shown by recent work of Chen and Yang [22], who also present data up to 30°. In that work, an 001 peak can clearly be seen still, indicating the sensitivity of the XRD technique in observing appropriate 001 peak, even though clay concentrations are below 5 wt%. However, as will be seen using TEM in the next paragraph, this lack of 001 peaks does not mean that the particles have fully delaminated but rather that they are well intercalated.

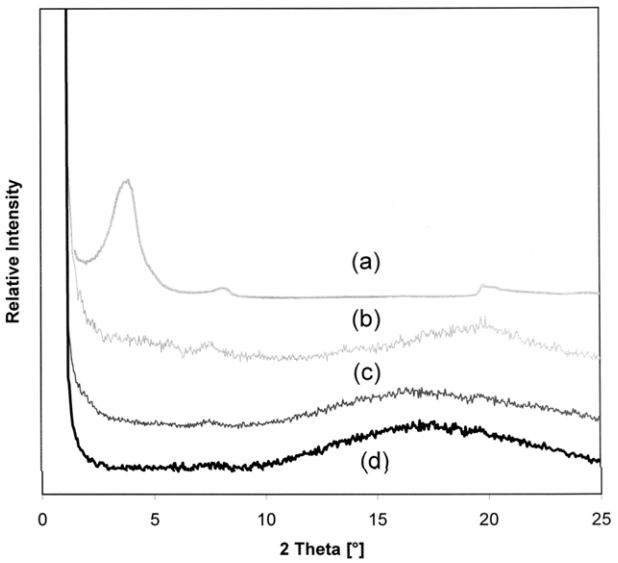

Fig. 2. X-ray spectra of: (a) clay, (b) DGEBA/clay, (c) HBP/clay and (d) DGEBA/HBP/clay.

The TEM photograph for the DGEBA–clay nanocomposite (Fig. 3a) indicates that tactoids or bundles of clay platelets still do exist, with spacings of approximately 90–100 Å determined from the micrographs. Clearly d-spacings of such size are too large (too low angles) to be observed in the X-ray diffraction experiments. Other micrographs of this material (not shown here) indicate that the length of the tactoids range from 200 to 1000 nm. Fig. 3b is of the HBP and layered silicate nanocomposite. It can be seen, as with DGEBA and clay, that tactoids readily exist even though no peaks are observed in the XRD spectra of Fig. 2. The quality of the micrograph is somewhat worse than Fig. 3a due to difficulties with cryo-microtoming this very rubbery sample, but it can be estimated that the spacing between layers is slightly greater (approximately 120 Å). Fig. 3c is of the HBP phase in DGEBA alone, where a phase separated HBP material exists in spheres of approximately 0.8–1 μm in diameter, as previously reported [19]. Micrographs of the ternary epoxy, HBP and layered silicate system showed distinct regions of clay tactoids and HBP phase-separated regions (no clay was observed in the HBP phase). Fig. 3d is of a phase-separated HBP region in the ternary system. The size of the phase-separated material appears similar, albeit a

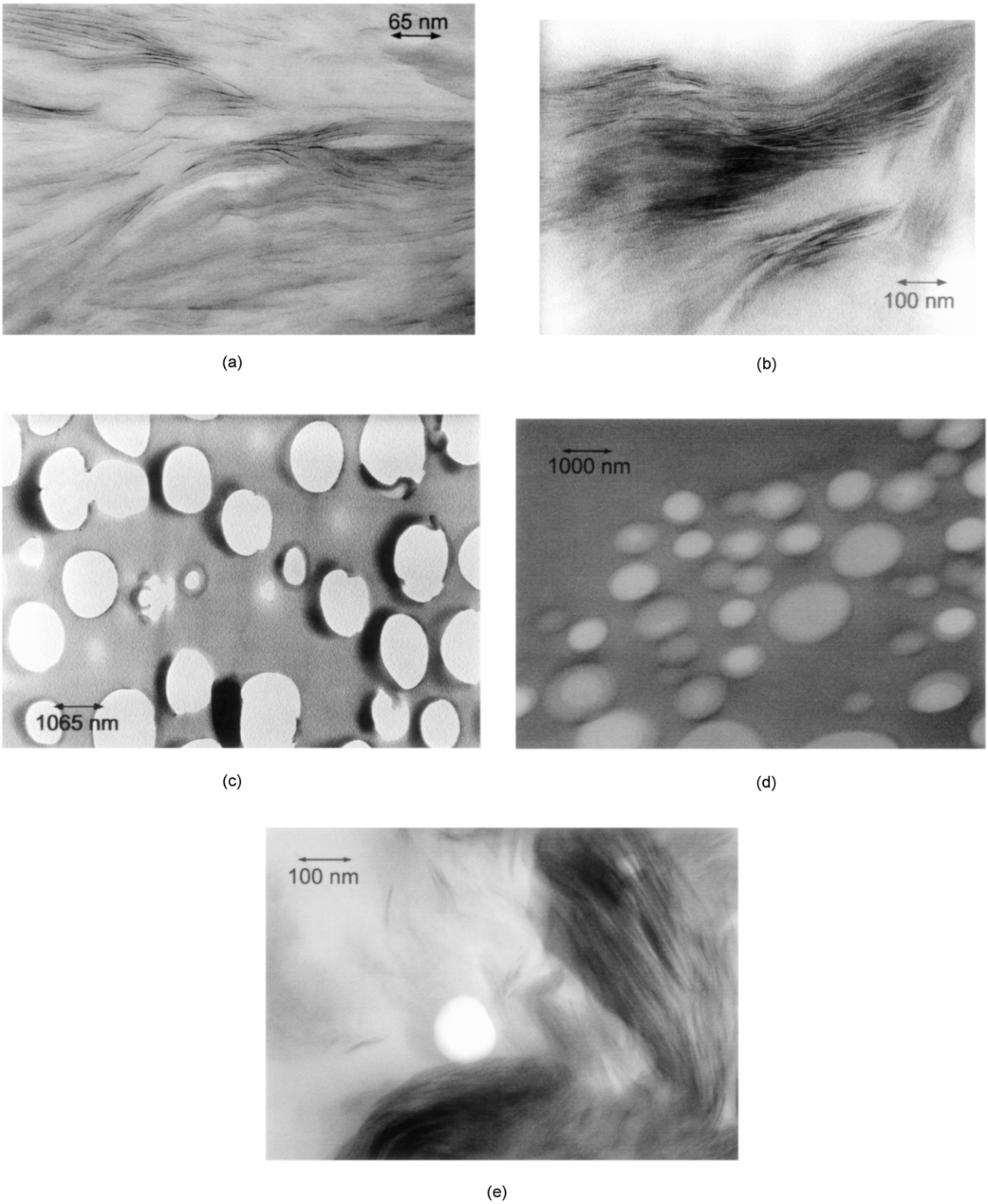

Fig. 3. TEM images of (a) HBP/clay, (b) DGEBA/HBP, (c) DGEBA/HDP, (d) DGEBA/HBP/clay (HBP region) and (e) DGEBA/HBP/clay (clay region).

little broader in size distribution, than binary blend HBP and epoxy, ranging between 300 and 1500 nm. Finally, Fig. 3e shows a clay tactoid in the ternary system. In this particular micrograph example, a very small phase-separated HBP particle can be seen to sit close to the tactoid. In summary then, the TEM micrographs indicate that despite a lack of 001 XRD reflections, clay forms intercalated tactoids in either DGEBA or HBP and HBP phase separates to particle

sizes of the order of 1 μm, either in DGEBA alone, or in the DGEBA/clay/HBP ternary system. That is, the presence of the clay has little effect on the phase separation of the HBP (albeit with a slightly broader size distribution). Thus in the ternary systems there exists distinct regions of clay tactoids, and HBP phase-separated regions.

The cured DGEBA, DGEBA/HBP blend and the two corresponding nanocomposites were subjected to DMTA analysis, both in the high temperature region of the rigid DGEBSA matrix (superambient) and in the region of the HBP loss peak (subambient). The loss factor vs. temperature and storage modulus vs. temperature plots are shown in Figs. 4 and 5, respectively, for the superambient measurement of the glass transition region of the DGEBA-rich phase. The nanocomposites show a slightly higher tanδ peak temperature compared to the corresponding matrix. This can be attributed to confinement of polymer chain as a result of intercalation into the interlayer gallery of the clay [17]. The lower T_g of DGEBA/HBP blend compared to pure DGEBA can be attributed to the presence of some extent of HBP which remains dissolved in the epoxy matrix [23,24].

Blending of HBP with epoxy results in a modest reduction in storage modulus whereas incorporation of clay results in significant increase in storage modulus. Hence the resultant modulus of epoxy/HBP/clay nanocomposite is significantly higher compared to the neat epoxy. An appropriate 50% increase in storage modulus was achieved as a result of incorporation of 5% of clay into the epoxy matrix. Although neither crosslinking density nor modulus of such exfoliated silicate layers are known, this behavior can be attributed to the very large

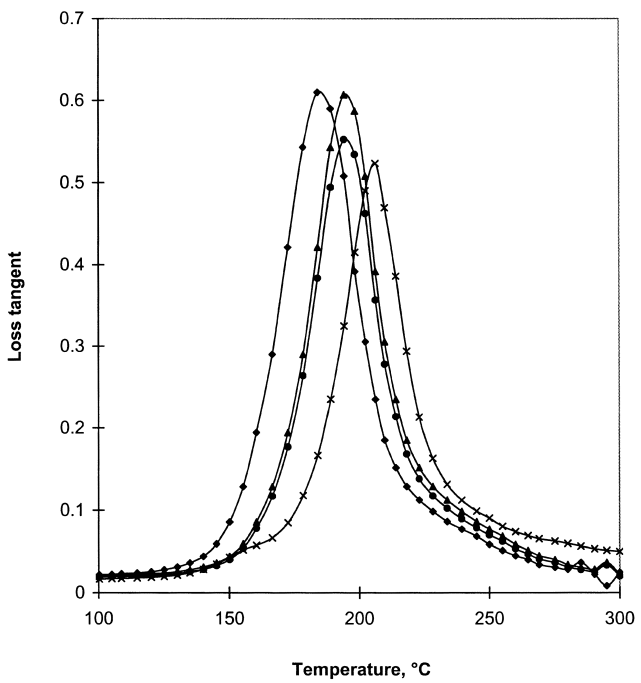

Fig. 4. Loss tangent vs. temperature (superambient) plots of cured networks: neat DGEBA (–▲–▲–), DGEBA/HBP (–■–■–), DGEBA/-clay (–x—x–) and DGEBA/HBP/clay (–●–●–).

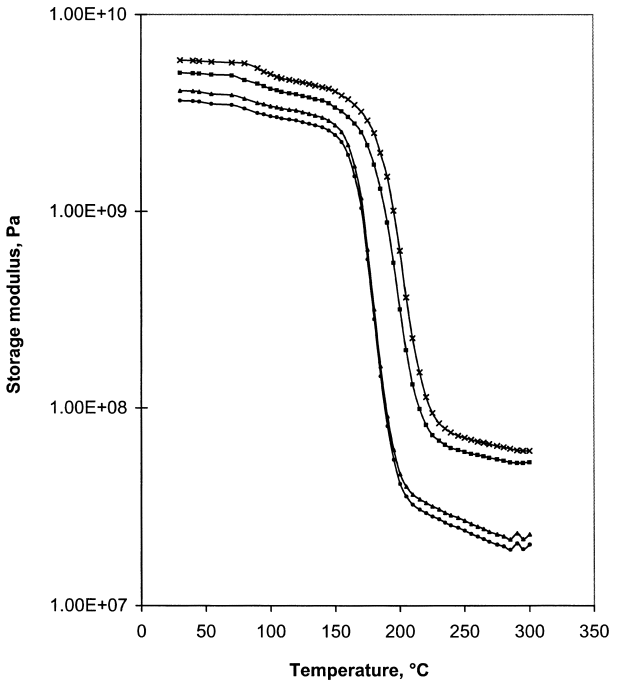

Fig. 5. Storage modulus vs. temperature (superambient) plots of cured networks: neat DGEBA (–▲–▲–), DGEBA/HBP (–●–●–), DGEBA/-clay (–x—x–) and DGEBA/HBP/clay (–■–■–).

aspect ratio of exfoliated silicate layers which is in the order of 1000 [25,26]. The increase in modulus is more prominent in the rubbery matrix. The rubbery plateau modulus of 5% clay containing nanocomposite is about three times higher than that of unfilled epoxy. This is a strong advantage of nanocomposite over the neat polymer in that it will be able to retain the high modulus even at a temperature above glass transition temperature (T_g). This indicates that clay modification is more effective in ridifying a flexible matrix compared to stiff one matrix. Similar observations have been reported in the literature using various epoxy matrices of different flexibilities [27,28].

Fig. 6 shows low temperature DMTA analysis on the materials containing HBP to study the state of that phase (namely, cured HBP, DGEBA/HBP HBP/clay, DGEBA/HBP/clay). In addition, the glass transition of the viscous HBP liquid prior to reaction was also determined (as outlined in Section 2, this was obtained using a different DMTA device) and was found to be −37 °C. It is clear from Fig. 6 that as has been shown earlier [20], the glass transition of the HBP phase in a cured, phase-separated DGEBA/HBP blend (ca. −43 °C) is somewhat lower than the glass transition of neat HBP, cured under the same conditions (ca. −11 °C) [20], yet slightly higher than the T_g of fully uncured HBP. The reason for this is not clear, but it has been postulated that it could be due to the nature of the partitioning of the amine in the phase-separating blend, with more amine remaining in the matrix DGEBA phase. The low temperature spectrum for DGEBA is also included as

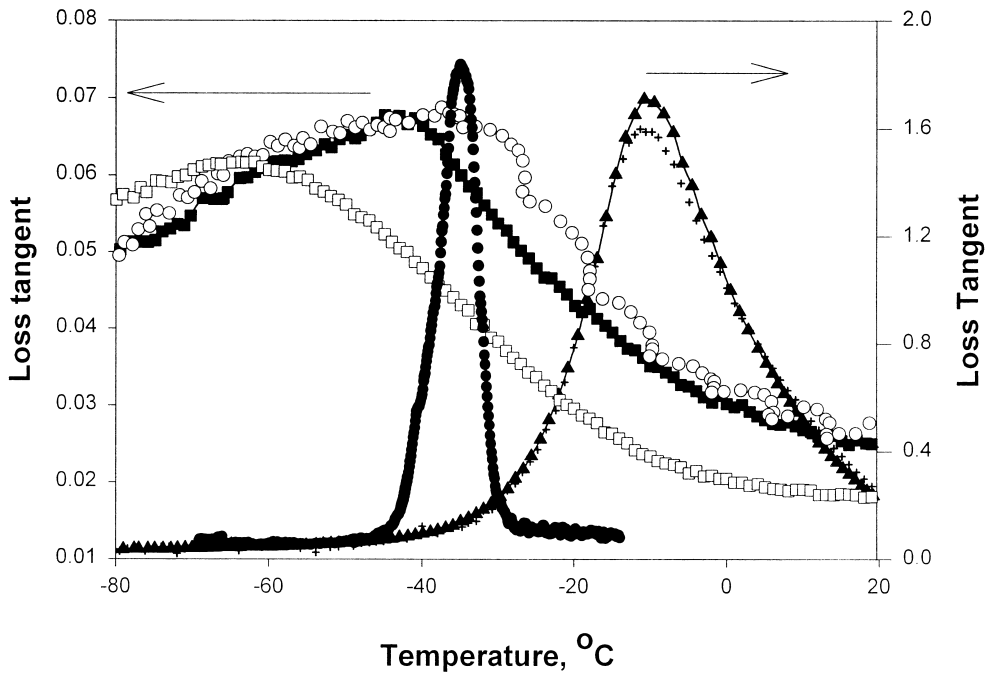

Fig. 6. Loss tangent vs. temperature (subambient) plots of cured networks: unreacted HBP (–●—●–), Neat cured HBP (–▲–▲–), DGEBA/HBP (–■–■–), HBP/clay (– + – + –) and DGEBA/HBP/clay (–○–○–), DGEBA (–□—□–).

DGEBA has a secondary relaxation which is often attributed to the glyceryl-like groups in DGEBA [29] but this peak is away from those of interest at about −65 °C. Thus from the DMTA results of Figs. 4 and 6, it is clear that the DGEBA/HBP blend is immiscible, with the HBP phase not being as fully cured when phase precipitated, it is when it is neat and mixed with amine.

Fig. 6 also shows that for cure of the HBP and amine, either without or in the presence of clay has little effect on the temperature location of the glass transition. The T_g of the HBP/clay nanocomposite is a few degrees less and the height slightly lower in magnitude, likely due largely to dilution effects of the clay. Interestingly, the glass transition of the HBP-separated phase in the ternary mixture of DGEBA/HBP/clay (−39 °C) is slightly greater than for HBP in the binary DGEBA/HBP material (−43 °C)—the presence of clay possibility stimulating further reaction.

The flexural and impact properties of the various epoxy matrices (neat DGEBA and DGEBA with the 15 wt% HBP) and their nanocomposites are shown in Table 1. Incorporation of HBP into epoxy matrix has little effect on flexural strength but a modest reduction in flexural modulus was observed. This can be attributed to the presence of low modulus HBP particles, as observed in many rubber modified epoxy systems [30,31]. The reinforcing effect of the clay, as expected from the incorporation of silicate layers, is reflected in higher flexural strength and modulus compared to the crosslinked DGEBA alone [26]. In spite of the reduction in flexural strength caused by HBP, DGEBA/HBP/clay nanocomposites show a significantly higher flexural strength and modulus compared to the neat epoxy, due to addition of the nanoclay.

Both the DGEBA/HBP and DGEBA/clay blend show a greater impact strength compared to the neat DGEBA. It could thus be expected that DGEBA/HBP/clay would show an even greater (synergistic) maximum impact strength. However, the impact strength of DGEBA/HBP/clay nanocomposite (1540 J/m) was lower than DGEBA/HBP blend (2250 J/m), though still higher than that of the neat epoxy (740 J/m), essentially being intermediate between them. The impact behavior can be explained from the SEM analysis of the fracture surface, as will be discussed shortly.

The SEM photomicrographs for the fracture surfaces of cured DGEBA, DGEBA/HBP, DGEBA/clay and DGEBA/HBP/clay are shown in Fig. 7. From the first micrograph for the case of unmodified epoxy (Fig. 7a), a smooth glassy

Table 1
Flexural and impact properties of HBP modified epoxy and nanocomposites

Blend composition epoxy/HBP/clay	Flexural strength (MPa)	Flexural modulus (MPa)	Impact strength (J/m)
100/0/0	112 ± 2	2900 ± 50	700 ± 50
100/15/0	109 ± 3	2500 ± 50	2200 ± 100
100/0/5	146 ± 5	5000 ± 50	1100 ± 150
100/15/5	135 ± 5	3650 ± 50	1500 ± 150

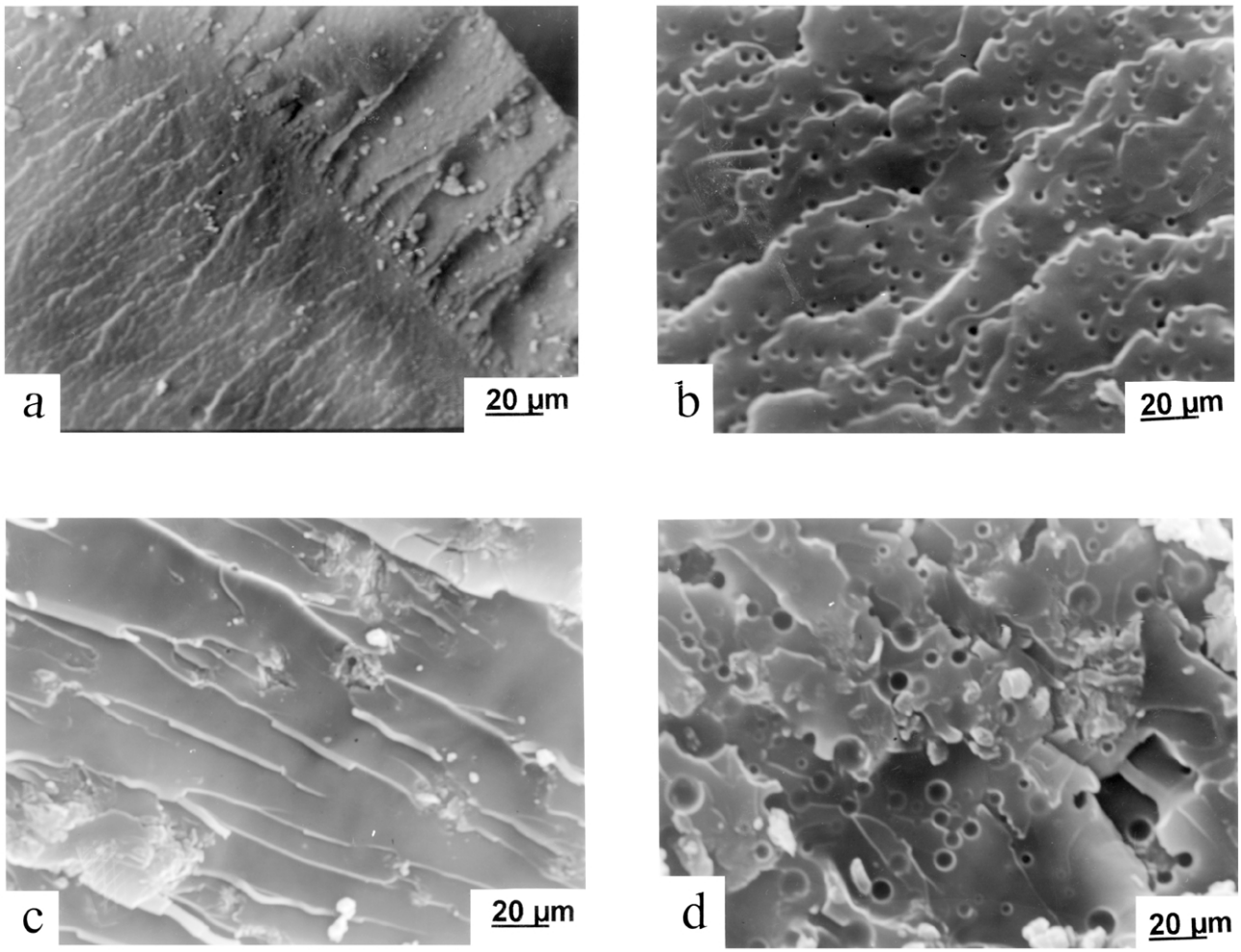

Fig. 7. SEM photographs for fracture surfaces of (a) neat DGEBA (b) DGEBA/HBP (c) DGEBA/clay (d) DGEBA/HBP/clay.

fractured surface occurs, with cracks in different planes can be seen. This indicates brittle fracture of the unmodified epoxy, which accounts for its poor impact strength. The fracture surfaces of the blend consists of two distinct phases, spherical HBP particles dispersed in a continuous DGEBA matrix, the particles have dimension in the range of 2–3 μm and their size distribution is bimodal in nature. The micrograph (Fig. 7b) shows the broken HBP particles and a stress-whitened zone. Stress whitening is due to the scattering of visible light from the layer of the scattering centers, which in this case are voids [32,33]. The generation of voids is due to the cavitation of rubbery HBP particles, which is an important energy dissipating mechanism in the case of rubber-toughened epoxies, both in itself [34,35], but more importantly because it encourages the yielding process to operate throughout the matrix [33–36].

The fracture surface of epoxy/clay nanocomposite (Fig. 7c) shows massive shear deformation. This indicates that upon exposure of mechanical stress, the stress concentrating nanoparticles appear to encourage shear yielding of the epoxy interlayers at the tip of the propagating crack, which continues throughout the entire volume. Energy is absorbed for such shear yielding leading to the increase in impact strength [37]. Shear of the clay layers thus seems likely.

It is also clear from the photograph (Fig. 7d) (as noted above, following TEM analysis) that the phase separation process is slightly affected due to the presence of clay. The uniformity of particle size and their distribution as observed in fracture surface of DGEBA/HBP blend is greater due to the presence of clay. This leads to a modest decrease in toughness as it is well known that uniform distribution of rubber particles is the key factor for toughening [33–36]. However, toughness is still greater than the use of just clay in DGEBA, or indeed DGEBA alone. Thus the use of a ternary mixture of epoxy/HBP and clay represents a good strategy to achieve a balance of modulus and toughness. The properties could likely be improved further with additional optimisation.

4. Conclusion

Nanocomposites based on epoxy and toughened epoxy formulation, were synthesized and characterized. Both the

strengthening and toughening of epoxy resin was achieved by incorporating HBP and clay. Strengthening effect of clay is slightly reduced by the presence of HBP. Although both the clay and HBP show a toughening effect, in the ternary blend, the net effect is less than that exerted by the HBP alone. However, the strategy represents a useful way to increase toughness and retain a significant modulus.

Acknowledgements

Dr Ratna is grateful to Department of Science and Technology for a BOYSCAST fellowship.

References

[1] Messersmith PB, Stupp SI. J Mater Res 1992;7:2559.
[2] Giannelis EB. Adv Mater 1996;8:29.
[3] Zilg C, Mulhaupt R, Finter J. Macromol Chem Phys 1999;200:661.
[4] Novak BM. Adv Mater 1993;5:422.
[5] Philipp G, Schimdt H. J Non-Cryst Solids 1984;80:283.
[6] Philipp G, Schimdt H. J Non-Cryst Solids 1986;82:31.
[7] Kakimoto M, Iyoku Y, Morikawa A, Yamaguchi H, Imai Y. Polym Prepr 1994;35:393.
[8] Ellsworth MW, Novak BM. Chem Mater 1993;5:839.
[9] Okada A, Usuki A. Mater Sci Engng 1995;C3:109.
[10] Usuki A, Kojima Y, Kawasumi M, Okoda A, Fukushima Y, Kurauchi T, Kamigaito O. J Mater Res 1993;8:1179.
[11] Usuki A, Kojima Y, Kawasumi M, Okoda A, Fukushima Y, Kurauchi T, Kamigaito O. J Mater Res 1993;8:1185.
[12] Kelly P, Akelah A, Qutubuddin S, Moet A. J Mater Sci 1994;29:2274.
[13] Weimer MW, Chen H, Giannelis EP, Sogah DY. J Am Chem Soc 1999;121:1615.
[14] Moet AS, Akelah A, Salahuddin N, Hiltner A, Baer E. Mater Res Symp Proc 1994;351:163.
[15] Wang Z, Massam J, Pinnavaia TJ. In: Pinnavaia TJ, Beall GW, editors. Polymer clay nanocomposites. New York: Wiley; 2000.
[16] LeBaron PC, Wang Z, Pinnavaia TJ. Appl Clay Sci 1999;15:11.
[17] Gilman JW, Kashiwagi T. In: Pinnavaia TJ, Beall GW, editors. Polymer clay nanocomposites. New York: Wiley; 2000.
[18] Messersmith PB, Giannelis EP. J Polym Sci, Part A, Polym Chem 1995;33:1049.
[19] Boogh L, Petersson B, Manson EJ. Polymer 1999;40:2249.
[20] Ratna D, Varley RJ, Singh Raman RK, Simon GP. J Mater Sci 2003; 38:147.
[21] Singh C, Balazs AC. Polym Int 2000;49:469.
[22] Chen KH, Yang SM. J Appl Polym Sci 2002;86:414.
[23] Manternal S, Pascault JP, Sautereau H. In: Riew CK, editor. Rubber toughened plastics. Advances in chemistry series, vol. 222. Washington, DC: American Chemical Society; 1989. p. 193.
[24] Pearson RA, Yee AF. J Mater Sci 1989;24:2571.
[25] Yano K, Usuki A, Kurauchi T, Kamigaito O. J Polym Sci Part A Polym Chem 1993;31:2000.
[26] Huang X, Lewis S, Brittain WJ, Vaia RA. Macromolecules 2000;3: 2000.
[27] Wang MS, Pinnavaia TJ. Chem Mater 1994;6:468.
[28] Lan T, Pinnavaia TJ. Chem Mater 1994;6:2216.
[29] Charlesworth JM. Polym Engng Sci 1988;28:221.
[30] Ratna D. Polymer 2001;42:4209.
[31] Ratna D, Banthia AK. Polym Int 2000;49:281.
[32] Chen TK, Jan YH. Polym Engng Sci 1994;34:778.
[33] Bascom WD, Hunston DL. In: Riew CK, editor. Rubber toughened plastics. Advances in chemistry series, vol. 222. Washington, DC: American Chemical Society; 1989. p. 135.
[34] Ratna D. Polym Int 2001;50:179.
[35] Kinloch AJ, Hunston DL. J Mater Sci Lett 1986;5:909.
[36] Bagheri R, Pearson RA. J Mater Sci 1996;31:3945.
[37] Kinloch AJ, Shaw SJ, Tod DA, Hunston DL. Polymer 1983;24:1355.